Control of the magnetic properties of n-type ferromagnetic semiconductor (In,Fe)As quantum wells using electric double layer transistor structure

Le Duc Anh[1]、Yuji Nakagawa[2]

[1]Department of Electrical Engineering and Information Systems, Tanaka-Ohya lab

[2]Department of Applied Physics, Iwasa lab

Abstract – (In,Fe)As is the first and the only n-type electron induced III-V ferromagnetic semiconductor so far, which possesses a very large s-d exchange interaction energy between electron carriers and Fe spins. For this reason, by controlling the carrier characteristics of the magnetic thin film using a field effect transistor structure, the magnetic properties of (In,Fe)As can be controlled isothermally, which is important for studying the magnetic physics as well as device applications. In this work we used electric double layer transistor (EDLT) structure to control the magnetic properties of (In,Fe)As quantum wells (QWs) capped with thin $(Al_{0.5}, Ga_{0.5})Sb$ layer. We observed high mobility (~ 1000 cm^2/Vs) and large negative magnetoresistance ($\sim 7.5\%$) in the (In,Fe)As QWs, which are much higher than those of the previous works. Although the effect of the gate voltage on the carrier characteristics was weak, we successfully controlled the magnitude of the magnetoresistance.

1. Authors information

Le Duc Anh – Specialty is semiconductor spintronics. In this research, he is in charge of sample growth, a part of EDLT device fabrication, and measurements of magnetic properties.

Yuji Nakagawa – Specialty is electrical transport measurement of layered materials. In this research, he is in charge of the other part of EDLT device fabrication, and measurements of electrical properties.

2. Introduction and the purposes of this work

The ferromagnetism of (In,Fe)As is induced by the s-d exchange interaction between electron carriers and Fe spins. Therefore in principle one can control the magnetic properties isothermally by controlling the carrier characteristics of the magnetic thin film using a transistor structure. This functionality of the material can be used in many device applications, such as non-volatile logic devices. In (In,Fe)As, a very large s-d exchange interaction energy was estimated, which indicates that the Curie temperature (T_C) can be increased up to room temperature provided a high enough electron concentration ($\sim 10^{20}$ cm^{-3}) can be obtained [1,2]. On the other hand, in the (In,Fe)As thin films where quantum size effect occurs [2], it is predicted that T_C will be quantized due to the quantization of the density of states in two-dimensional systems [3]. Therefore, it is important, from the viewpoints of both magnetic physics and device technology, to study the behavior of the magnetic properties of (In,Fe)As quantum wells when the carrier density is changed in a wide range.

In our previous work [4], we have used the electric double layer transistor (EDLT) to control the T_C of InAs/(In,Fe)As/InAs trilayer surface QWs. The change of sheet carrier density (Δn_{sheet}) of the QWs, however, was at most only 2×10^{12} cm^{-2}. This Δn_{sheet} is smaller by $1-2$ orders of magnitude than those reported in oxide thin films or Van der Waals layered crystals using the same device structure [5,6]. Moreover, it seemed that the closer the

(In,Fe)As layer was placed to the surface, the smaller Δn_{sheet} was obtained. This indicated a possibility that the Fe atoms diffused to the surface and created impurity states that strongly pinned the Fermi level of the (In,Fe)As QWs. A solution to this problem is to insert a cap layer in the surface of the (In,Fe)As QWs. This design, however, also separates the electron carriers accumulated at the surface from the Fe local spins in the (In,Fe)As layer and weakens the gating effect of the magnetic properties.

In this self-directed joint research, we aim to solve this dilemma by capping the (In,Fe)As QWs with a $(Al_{0.5},Ga_{0.5})Sb$ thin film, as shown in Fig. 1A. In this structure design, the (In,Fe)As layer is placed further from the surface. Meanwhile, as shown in Fig. 1B, due to the high conduction band offset at the $(Al_{0.5},Ga_{0.5})Sb/(In,Fe)As$ interface (1.1 eV), the electron carriers that are accumulated at the surface will be transferred into the (In,Fe)As QW. Moreover, $(Al_{0.5},Ga_{0.5})Sb$ and (In,Fe)As have almost the same lattice constant (about 6.1 Å), thus the heterostructure in Fig. 1A can be epitaxially grown without much difficulty. As the huge capacitance of EDLT is due to the ultrathin thickness of the electrical double layer (equal to the ion-size), inserting a cap layer would hinder the gating effect. However, it has been reported that large Δn_{sheet} is still possible if the cap layer thickness is in the order of several nm [7]. Thus there should be an optimal thickness of the $(Al_{0.5},Ga_{0.5})Sb$ cap layer where the largest gating effect of the (In,Fe)As QW can be obtained.

Here, we study the control of magnetic properties of (In,Fe)As QWs capped with thin $(Al_{0.5},Ga_{0.5})Sb$ layers by the gate voltage in EDLT structures. By varying the thickness of the cap layer, we would like to determine the optimal thickness for the gating effect, and investigate the behavior of the magnetic properties of (In,Fe)As QWs in those devices.

3.   Experimental results

3.1 Sample growth

The samples in this study were grown by molecular beam epitaxy (MBE). The sample structure is illustrated in Fig 1A, with the top layers are $(Al_{0.5},Ga_{0.5})Sb$ (t nm)/(In,Fe)As (10 nm, Fe 6%)/InAs (5 nm). Note that the $(Al_{0.5},Ga_{0.5})Sb/(In,Fe)As$ layers had to be grown at low temperature (~236℃) to prevent the segregation of Fe atoms. We prepared 3 samples A, B, and C with $t = 2, 5, 10$ nm, respectively. Figure 1C shows the *in-situ* reflection high energy electron diffraction (RHEED) patterns of the three samples. The RHEED patterns indicate the best growth conditions for sample B. In sample C, we observed a dim amorphous ring in the RHEED pattern, indicating degradation of the crystal quality of the cap layer.
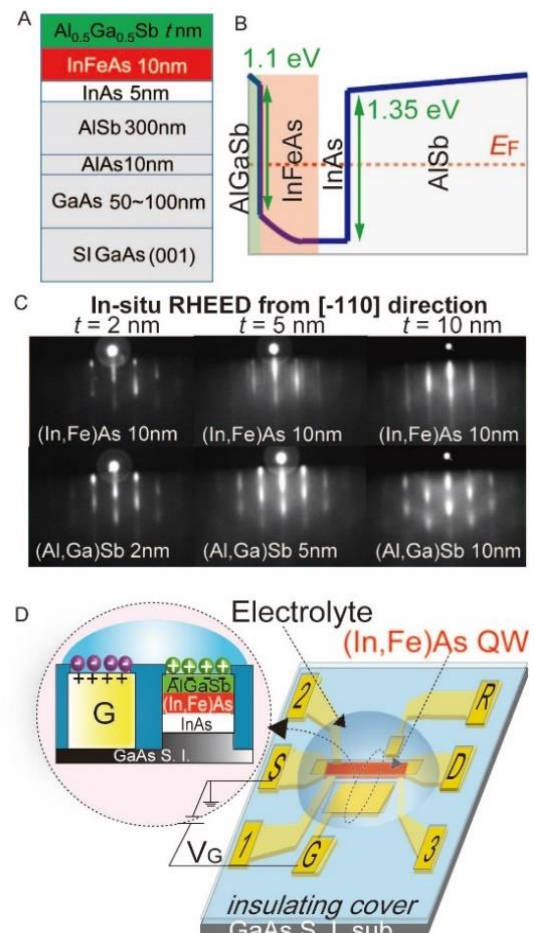

Fig 1. A. Sample structure. B. Potential profile of the conduction band of the heterostructure in A. C. *in-situ* RHEED patterns during the MBE growth. D. The plane-view of the EDLT devices

2

3.2.   Fabrication of EDLT devices

Figure 1D shows the plane-view of our EDLT devices. The samples were etched into 50×200 μm^2 Hall bars using standard photolithography and ion milling. Side gate (G), source (S), drain (D) and electrodes for transport measurements were formed by vacuum evaporation of Cr (5 nm)/Au (50 nm) and lift-off technique. The whole area was passivated by an insulating resist cover, and contact holes were opened on the surface of the Hall bar, the side gate G, and metal electrodes. Finally ion liquid (DEME-TFSI) was put on top of the Hall bar and the gate G to form the EDLT. When a positive V_G is applied, ions in the ion liquid accumulate at the surface of the semiconductor channel and form an electric double-layer capacitor, which changes the potential and electron density in the (In,Fe)As/InAs QW.
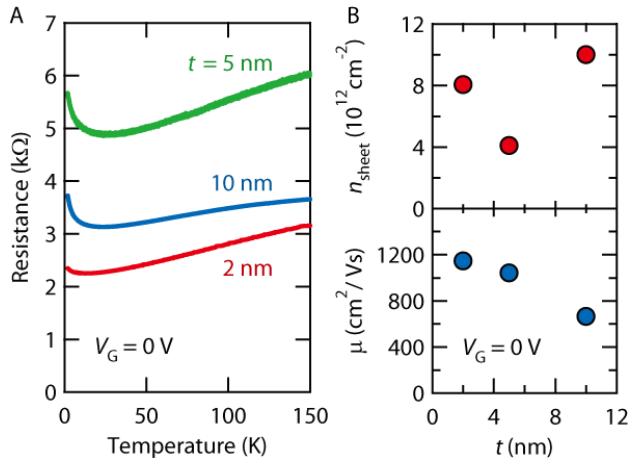
3.3.   Transport properties

Fig. 2. Transport properties of samples A, B, C at V_G = 0 V. A. Temperature dependence of resistance. B. Sheet electron density n_{sheet} (top panel), measured at 2 K, and mobility μ, measured at 20 K (bottom panel).

Figure 2 shows the transport properties of sample A, B, and C at V_G = 0 V. The temperature dependence of resistance (R-T curves) of the three samples show metallic behavior, but slightly turn upward below 20 K. Figure 2B shows the sheet electron density n_{sheet}, estimated from the

normal Hall resistance at 2 K, and mobility μ, estimated at 20 K, of the three samples. The n_{sheet} value is smallest in sample B (t = 5 nm), while the mobility μ monotonically decreases from 1140 cm^2/Vs (t = 2 nm) in sample A to 660 cm^2/Vs in sample C (t = 10 nm). The mobility in all the samples are, however, much higher than that in the previous study (200 cm^2/Vs) [4].

Without any intentional doping, the electron carriers in these (In,Fe)As QWs were generated from crystal defects. From the band profile in Fig. 1B, one can see that the carriers generated from defects in the $(Al_{0.5},Ga_{0.5})$Sb cap layers would be transferred into the (In,Fe)As QWs. As a result, the n_{sheet} of the QWs depends strongly on the crystal quality of the cap layers. n_{sheet} is smallest in sample B (t = 5 nm) and highest in sample C (t = 10 nm), consistent with the crystal quality deduced from the RHEED patterns. On the other hand, the separation of the ionized defects (in the cap layers) and the electron carriers (in the QWs) is likely the reason for relatively high mobility in all the three samples.

From Fig.2B, it is notable that the mobility μ is higher in sample with thinner cap layer. The crystal quality of the cap layer is a factor that affect μ, as electron carriers are scattered at the $(Al_{0.5},Ga_{0.5})$Sb/(In,Fe)As interface. This caused the remarkable decrease of μ in sample C, where the crystal quality of the cap layer is worst. The mobility can also be affected by the absorption of ions in the ion liquid into the ionized surface states, which occurs even at V_G = 0. This effect compensates the scattering of electron by ionized centers in the cap layer, leading to higher mobility in sample with thinner cap layer. However, in order to confirm this effect a comparison of the mobility values before and after dropping the ion liquid is required.

Next, we study the gating effect on the transport properties. Figure 3A shows the change of the source – drain current (I_{DS}) when applying the gate voltage V_G. The I_{DS} values were normalized to the value at V_G = 0. The change of I_{DS} was only 2 – 3%, the same order with that of

the previous work [4]. The change of the source – drain resistance was very small in the whole range of temperature, as shown in Fig. 3B. Figure 3C summarizes the change of n_{sheet} and μ of the three devices. Except the device C (t = 10 nm), the change of n_{sheet} and μ was almost negligible.

The gating effect in the ELDT devices of the three samples was very weak, which is opposite to our expectation. The ions might not accumulate on the cap surface, or the induced carriers were trapped into the defects of the cap layers. If it was the former, optimization of the ion liquid would be required. If it was the latter, using other materials, such as MgO or hexagonal BN, for the cap layer is worth investigating.
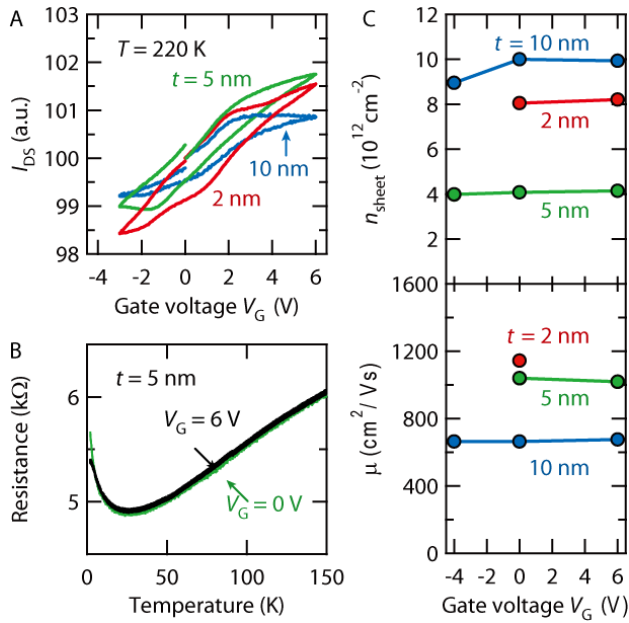

Fig 3. A. Variation of the source – drain current (I_{DS}) when applying V_G. B. Temperature dependence of the source – drain resistance when applying V_G = 0 and 6 V. C. the change of n_{sheet} and μ of the three devices with V_G.

3.4. Magnetic properties

3.4.1. Magnetization

Figure 4A shows the magnetic field dependence of anomalous Hall resistance (AHR – H curves) of sample B (t = 5 nm), measured at increasing temperatures. At 4.2 K,

the AHR shows ferromagnetic hysteresis. When increasing the temperature above 7 K, the hysteresis disappeared and the AHR – H curves became linear. These results indicate a $T_C \sim$ 5K in this sample. Figure 4B shows the AHR – H curves of sample B measured at 4.2 K under V_G = 0 V and 4 V. Almost no difference was observed, which was expected as the gating effect was very weak. The same results were obtained for the EDLT devices of samples A and C.
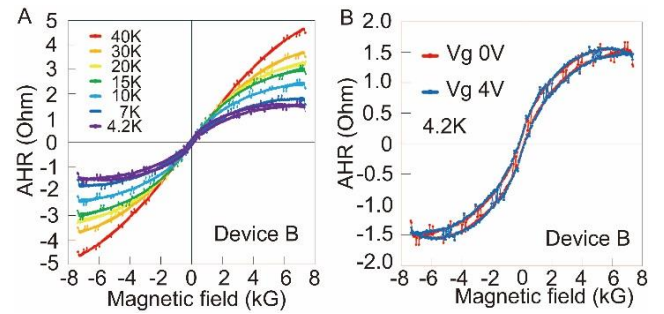

Fig. 4. A. The magnetic field dependence of the anomalous Hall resistance (AHR – H curves) of sample B at various temperatures. B. AHR – H curves of sample B at V_G = 0 V and 4 V, at 4.2 K.

3.4.2. Large magnetoresistance

Figure 5A shows the magnetoresistance (MR) of sample A, B, and C, measured at 4.2 K. All the samples show negative MR with the magnitude of several %. Under a magnetic field of 7.5 kG, MR of samples A, B, C are 2.3, 7.5, 4.4%, respectively. The MR magnitude seems to be larger in the QW with smaller n_{sheet}.

The change of MR with applying V_G of samples A and B are shown in Fig. 5B. The corresponding change of n_{sheet} of the QWs in samples A and B are summarized in Fig. 5C. Although the change of n_{sheet} was very small ($< 2 \times 10^{11}$ cm^{-2}), we observed clear changes of MR in both devices. Again, the MR magnitude seems to decrease with increasing n_{sheet} of the devices.
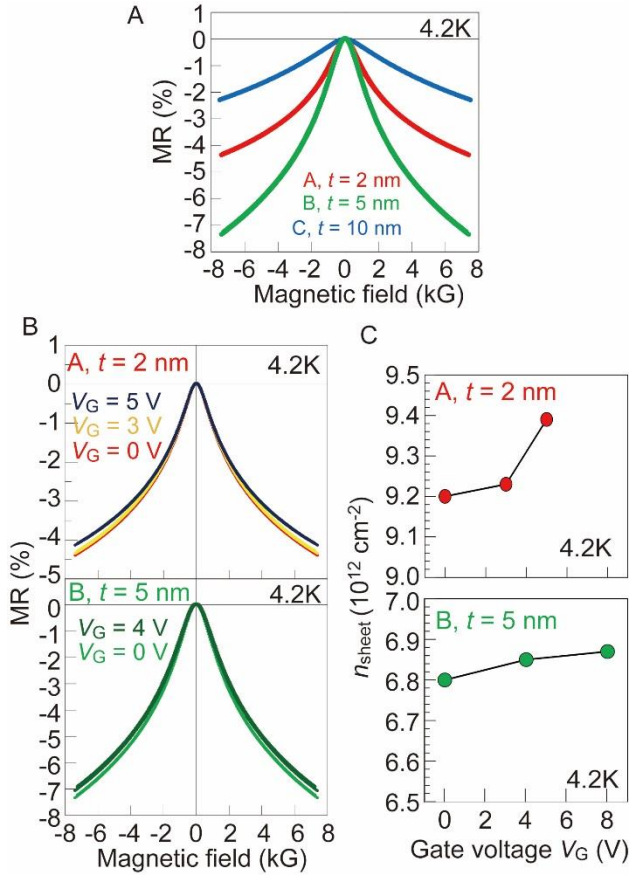
Fig. 5. A. Magnetoresistance (MR) of samples A, B, C measured at 4.2 K. B,C. The change of MR and sheet electron density n_{sheet} of sample A and B with the gate voltage V_G, respectively, at 4.2 K .

The negative MR is typical for ferromagnetic semiconductors, and has been observed in bulk-like (In,Fe)As samples. However, the magnitude of the negative MR in the bulk-like samples was at most 0.5% [8]. Thus the MR in the (In,Fe)As QWs under study is larger by one order of magnitude than that of the thick samples. The origin of negative MR is usually attributed to the spin-disorder scattering mechanism: When the local spin of Fe atoms are aligned by the external magnetic field, the scattering of electron carriers at these local spins is suppressed, leading to lower resistivity. The MR magnitude is given as the Khosla – Fischer equations [9]:

$$\frac{\Delta\rho}{\rho_0} = -B_1\ln(1 + B_2^2 H^2) \tag{1}$$

$$B_1 = A_1 J \rho_F [S(S+1) + \langle M^2 \rangle] \tag{2}$$

$$B_2^2 = \left[1 + 4S^2\pi^2\left(\frac{2J\rho_F}{g_0}\right)^4\right]\frac{g_0^2\mu^2}{(\alpha kT)^2} \tag{3}$$

Here $\frac{\Delta\rho}{\rho_0}$ is the MR ratio, A_1 is a constant, J is the s-d exchange interaction integral, ρ_F is the density of states at the Fermi level, S is the spin momentum of Fe atom (=5/2), M is the local magnetization, g_0 is the Lande factor, μ is the Bohr magneton, k is the Boltzmann constant, T is the absolute temperature, and α is a constant in the order of 1. From these equations, since the magnetization M is almost unchanged with V_G (Fig. 4), the change of MR magnitude of a single device under V_G can be attributed to the change of $J\rho_F$. On the other hand, in (In,Fe)As QWs the density of states ρ_F is quantized. Therefore, within the very small change of n_{sheet} the ρ_F value will not change. Thus from the Khosla – Fischer equations the change of MR with V_G likely reflects the change of the s-d exchange interaction J. Similarly, the large MR magnitude in the (In,Fe)As QWs under study comparing to that of the bulk-like samples may indicate an enhancement of the s-d exchange interaction J in low-dimensional magnetic systems. This enhancement effect of the s,p-d exchange interactions in low-dimensional systems was proposed theoretically [10]. On the other hand, the dependence of s-d exchange interaction energy in the QW on the QW thickness and the confinement potential has been observed in p-type (Ga,Mn)As [11]. Thus there is a possibility that the electrical control of MR in the EDLT devices of samples A and B is the result of the change of the s-d exchange interaction energy caused by the change of the QW confinement potential. If this is the case, the MR magnitude provides us a good probing tool for the s-d exchange interaction and the effect of electrical gating on this important physical quantity.

However, the Khosla – Fischer equations (1-3) was built for the three-dimensional magnetic systems, which cannot be aplied for the (In,Fe)As QWs without any modifications. It was shown that in the two dimensional

magnetic systems the movement of the carrier wavefunctions with V_G yields important effects on the magnetic properties such as magnetization and T_C [2,4]. Therefore, a correction of the Khosla – Fischer model for two dimensional magnetic systems is strongly required for a better understanding of the experimental results.

4.   Summary and outlook

In this self-directed joint research, we have fabricated the EDLT devices of (In,Fe)As QW capped with a thin $(Al_{0.5},Ga_{0.5})Sb$ layer (thickness t = 2,5,10 nm), and evaluated the gating effect on the transport and magnetic properties of the (In,Fe)As QWs.

The (In,Fe)As QWs capped with $(Al_{0.5},Ga_{0.5})Sb$ all show high mobility (~1000 cm^2/Vs), which was explained by the separation of the ionized defects from the conducting channel. The mobility and sheet electron density of the (In,Fe)As QWs strongly depend on the crystal quality of the $(Al_{0.5},Ga_{0.5})Sb$ cap layers. Although all the samples have low T_C (~5K), they exhibited negative MR that is larger than those in bulk-like samples by one order of magnitude.

The gating effect in the ELDT devices of the three samples was very weak, which is opposite to our expectation. Optimization of the ion liquid, or using other materials, such as MgO or hexagonal BN, for the cap layer are necessary. However, we observed clear change in the negative MR of the (In,Fe)As QWs with the gate voltage. The origin of the effect is unclear at this stage, but the change of the *s-d* exchange interaction energy due to the deformation of the confinement potential, or the movement of the carrier wavefunctions inside the QWs were proposed as the possible mechanisms. A control of the carrier characteristics in a much wider range, and a model for magnetoresistance of two-dimensional magnetic systems are strongly required for further understanding.

6.   References

1. P. N. Hai, L. D. Anh, M. Tanaka, Appl. Phys. Lett. **101,** 252410 (2012).

2. L. D. Anh, P. N. Hai, M. Tanaka, Appl. Phys. Lett. **104,** 046404 (2014).

3. N. Kim, J. W. Kim, S. J. Lee, Y. Shon, T. W. Kang, G. Ihm and T. F. George, Journal of Superconductivity: Incorporating Novel Magn. **18**, p. 189, (2005).

4. L. D. Anh, P. N. Hai, Y. Kasahara, Y. Iwasa, M. Tanaka, Phys. Rev. B **92**, 161201(R) (2015).

5. K. Ueno, S. Nakamura, H. Shimotani, et al. Nat Mater **7**, 855 (2008).

6. J. T. Ye, S. Inoue, K. Kobayashi, et al. Nat Mater **9**,125 (2010).

7. P. Gallagher, M. Lee, T. Petach, et al. Nat Commun **6**, 6437 (2015).

8. P. N. Hai, L. D. Anh, S. Mohan, T. Tamegai, M. Kodzuka, T. Ohkubo, K. Hono, M. Tanaka, Appl. Phys. Lett. **101,** 182403 (2012).

9. R. P. Khosla and J. R. Fischer, Phys. Rev. B **2**, 4084 (1970).

10. T. Dietl, A. Haury, Y. Merle d'Aubigne, Phys. Rev. B **55**, R3347 (1997).

11. N. P. Stern, R. C. Myers, M. Poggio, A. C. Gossard, and D. D. Awschalom, Phys. Rev. B **75**, 045329 (2007).